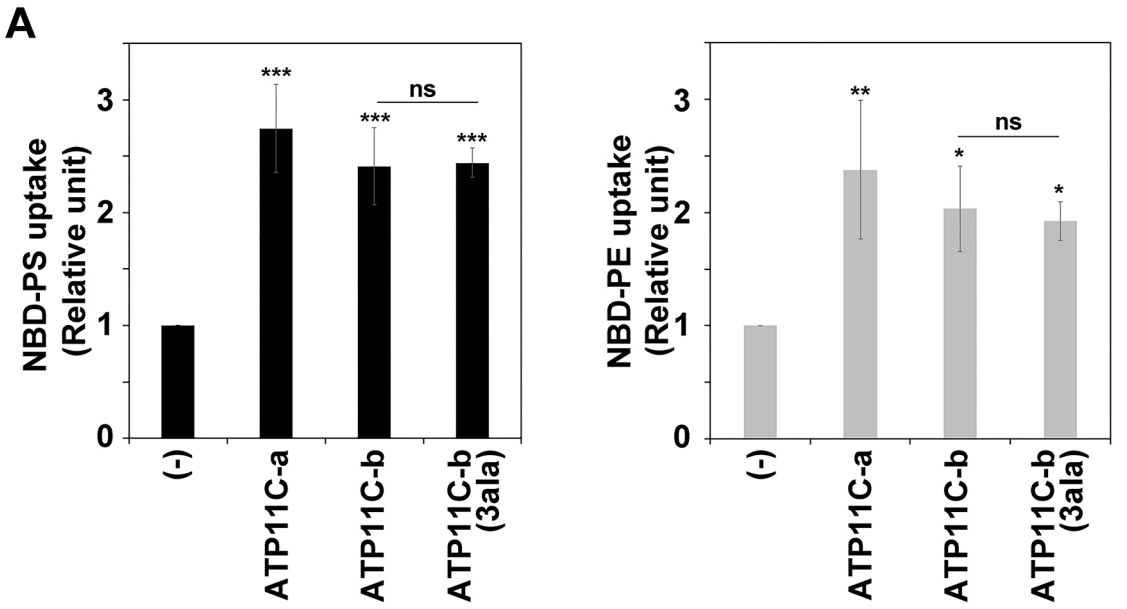

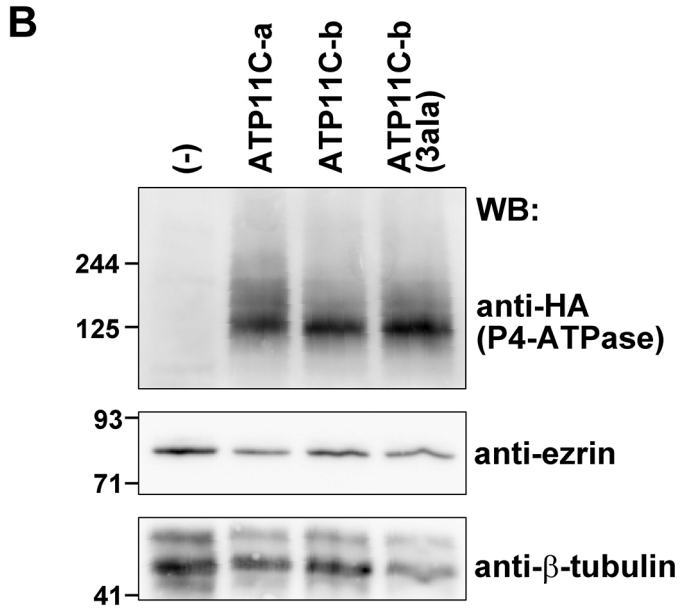

Supplementary Figure S1 Inoue & Takatsu

Fig. S1. Comparison of flippase activity between ATP11C-a, ATP11C-b, and ATP11C-b(3ala)-expressing cells. (A) Parental MDA-MB-231 cells (-) and MDA-MB- 231 cells stably expressing ATP11C-a, ATP11C-b, or ATP11C-b(3ala) were washed with flippase assay buffer and incubated with NBD-labelled lipids (NBD-PS for 5 min or NBE-PE for 15 min) at 15°C. After extraction with fatty acid-free BSA, the residual fluorescence intensity of the cells was measured by flow cytometry. Uptake of NBD-labelled lipids is shown relative to parental cells (-). Graphs ± SD display the average of three independent experiments. Variance was assessed by comparison of all pairs using a Student's *t*-test. * $p < 0.05$, ** $p < 0.01$, *** $p < 0.001$, ns not significant. **(B)** MDA-MB- 231 cells stably expressing ATP11C-a, ATP11C-b, or ATP11C-b(3ala), and parental cells (-), were lysed and subjected to immunoblotting using anti-H A, anti-ezrin, or anti-β-actin antibodies.

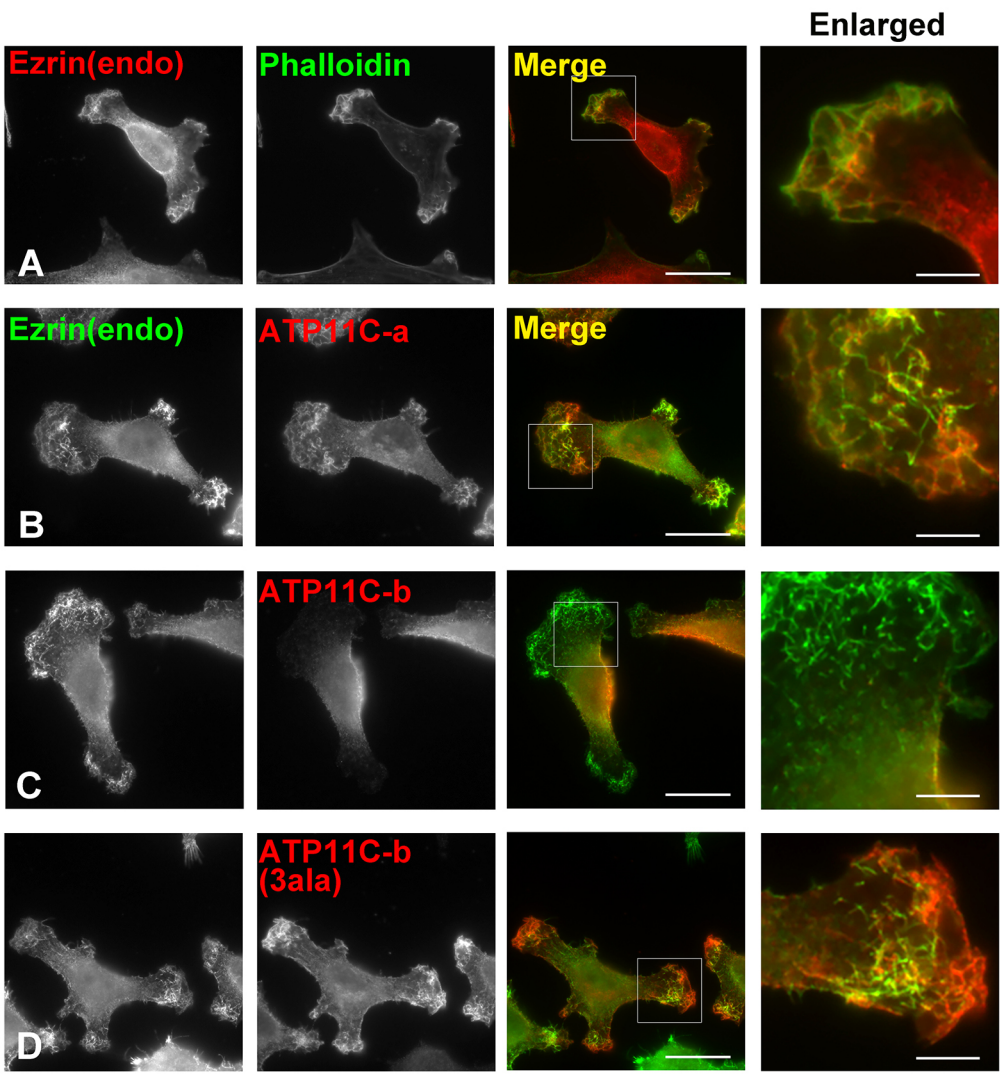

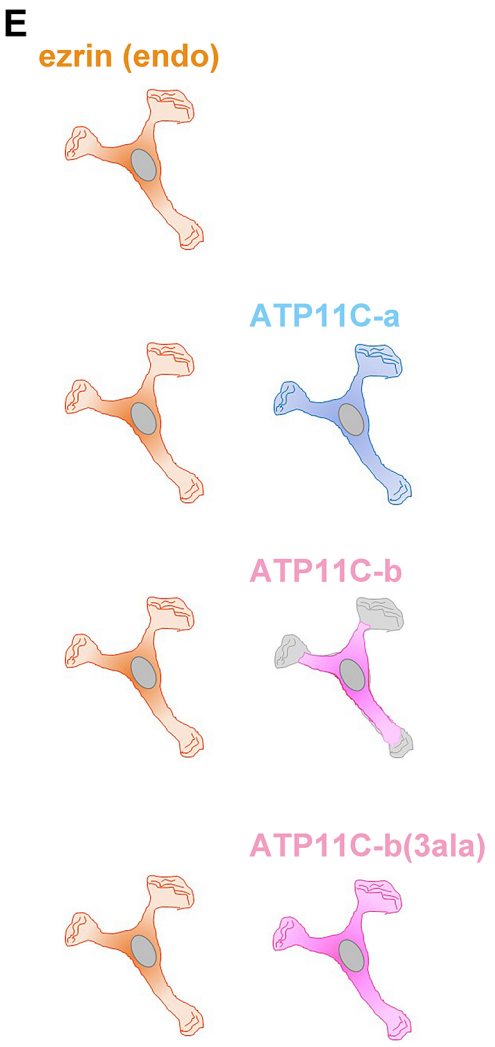

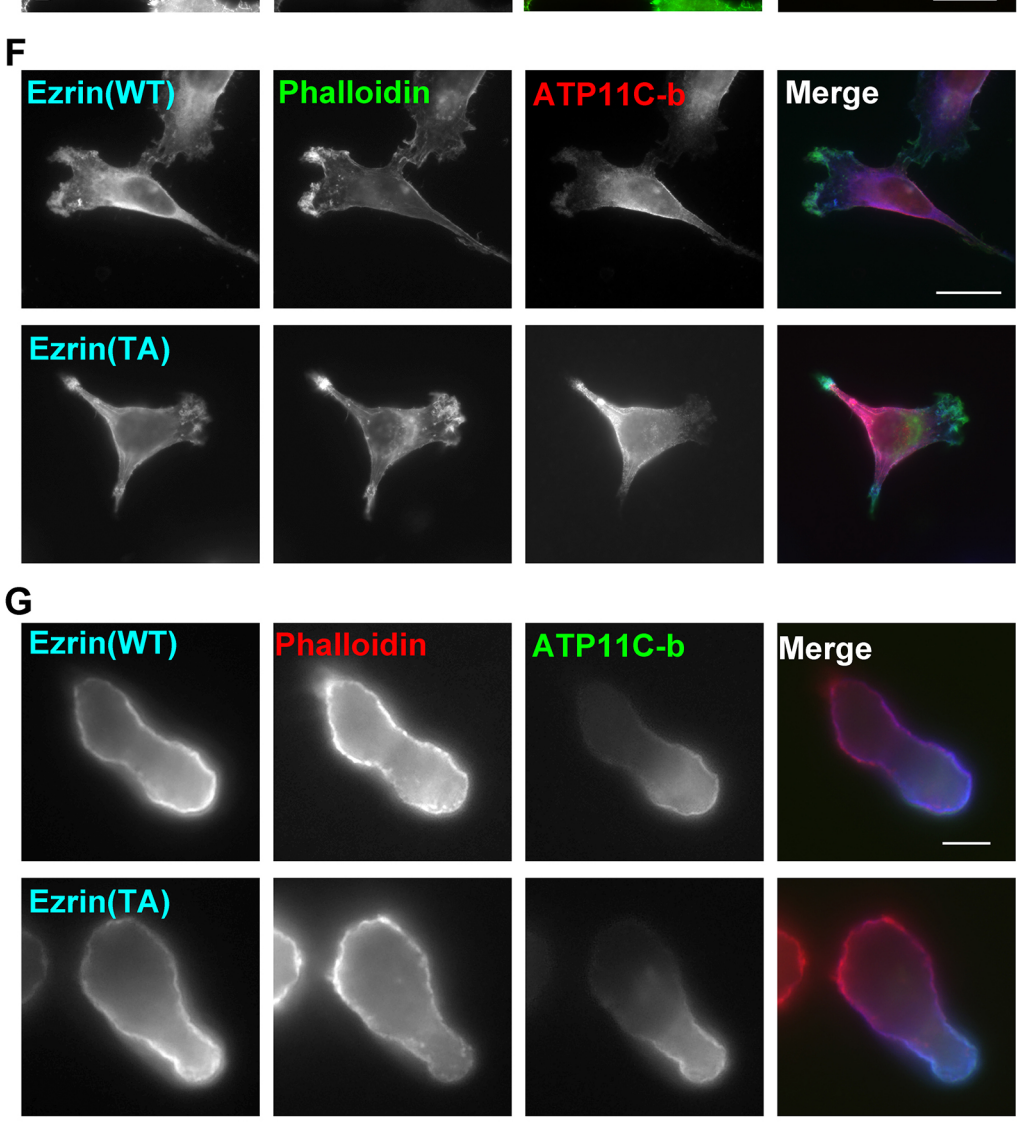

Supplementary Figure S2 Inoue & Takatsu

Fig. S2. Localization of endogenous ezrin in cells expressing ATP11C-a, ATP11C-b, or ATP11C-b(3ala). (A) Parental MDA-MB-231 cells (-) and MDA-MB-231 cells stably expressing **(B)** ATP11C-a, **(C)** ATP11C-b, or **(D)** ATP11C-b(3ala) were fixed and immunostained using anti-ezrin alone **(A)** or anti-ezrin and anti-HA antibodies **(B-D)** followed by incubation with Alexa555-conjugated anti-mouse secondary antibody and Alexa488-conjugated phalloidin **(A)** or Alexa488-conjugated anti-mouse and Cy3-conjugated anti-rat secondary antibodies **(B-D)**. Scale bars, 20 μm. Scale bars in enlarged images, 5 μm. **(E)** Schematic illustration of localization of endogenous ezrin and each ATP11C isoform and corresponding mutants. Orange, endogenous ezrin; light blue, ATP11C-a; pink, ATP11C-b. **(F)** MDA-MB-231 cells and **(G)** BaF3 cells stably co-expressing HA-tagged ATP11C-b and FLAG-tagged ezrin(WT) or ezrin(T567A) (TA) were fixed and stained for HA and FLAG followed by incubation with Cy3-conjugated anti-rat and DyLight649-conjugated anti-mouse secondary antibodies and Alexa488-conjugated phalloidin **(F)**, or Alexa488-conjugated anti-rat and DyLight649-conjugated anti-mouse secondary antibody and Alexa555-conjugated phalloidin **(G)**. Scale bars, 20 μm **(F)** and 5 μm **(G).**

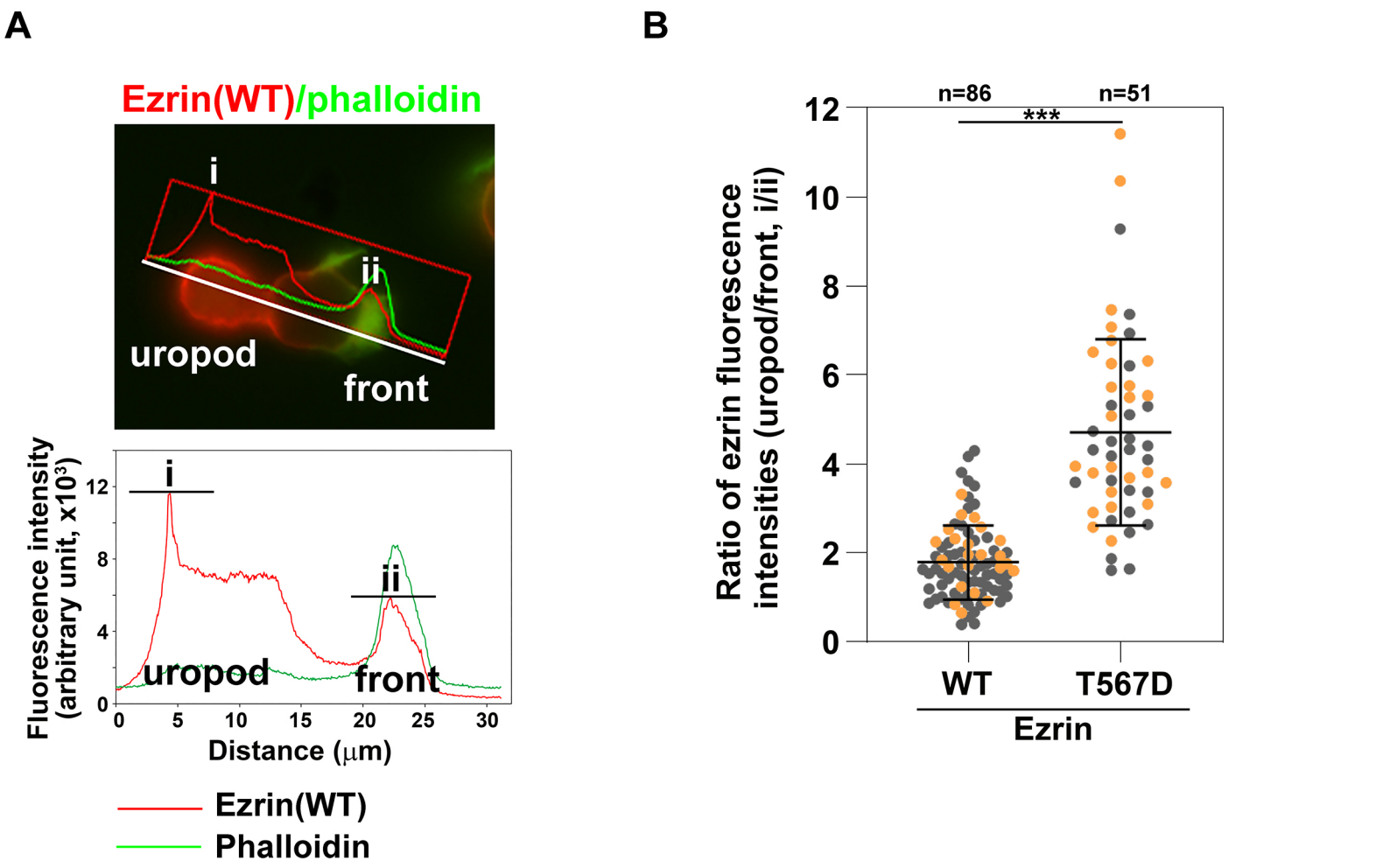

Supplementary Figure S3 Inoue & Takatsu

Fig. S3. Estimation of polarized localization of ezrin(WT) and the phosphomimetic ezrin mutant. (A) A representative line-scan profile from the uropod to the front of a BaF3 cell expressing ezrin(WT). The line scan was performed using the ZEN software. **(B)** The ratio of the peak fluorescence intensity of the uropod to front (i/ii) of a BaF3 cell expressing ezrin(WT) or ezrin(T567D) was calculated and expressed as scatter plots, as described in the legend for Figure 6D. Individual dots represent the ratios in individual cells. Graphs ± SD display the average ratio from all analyzed cells, and 'n' is the total number of analyzed cells from two independent experiments. Variance was assessed by comparison between ezrin(WT) and ezrin(T567D) using a Student's *t*-test. *** $p < 0.0001$.

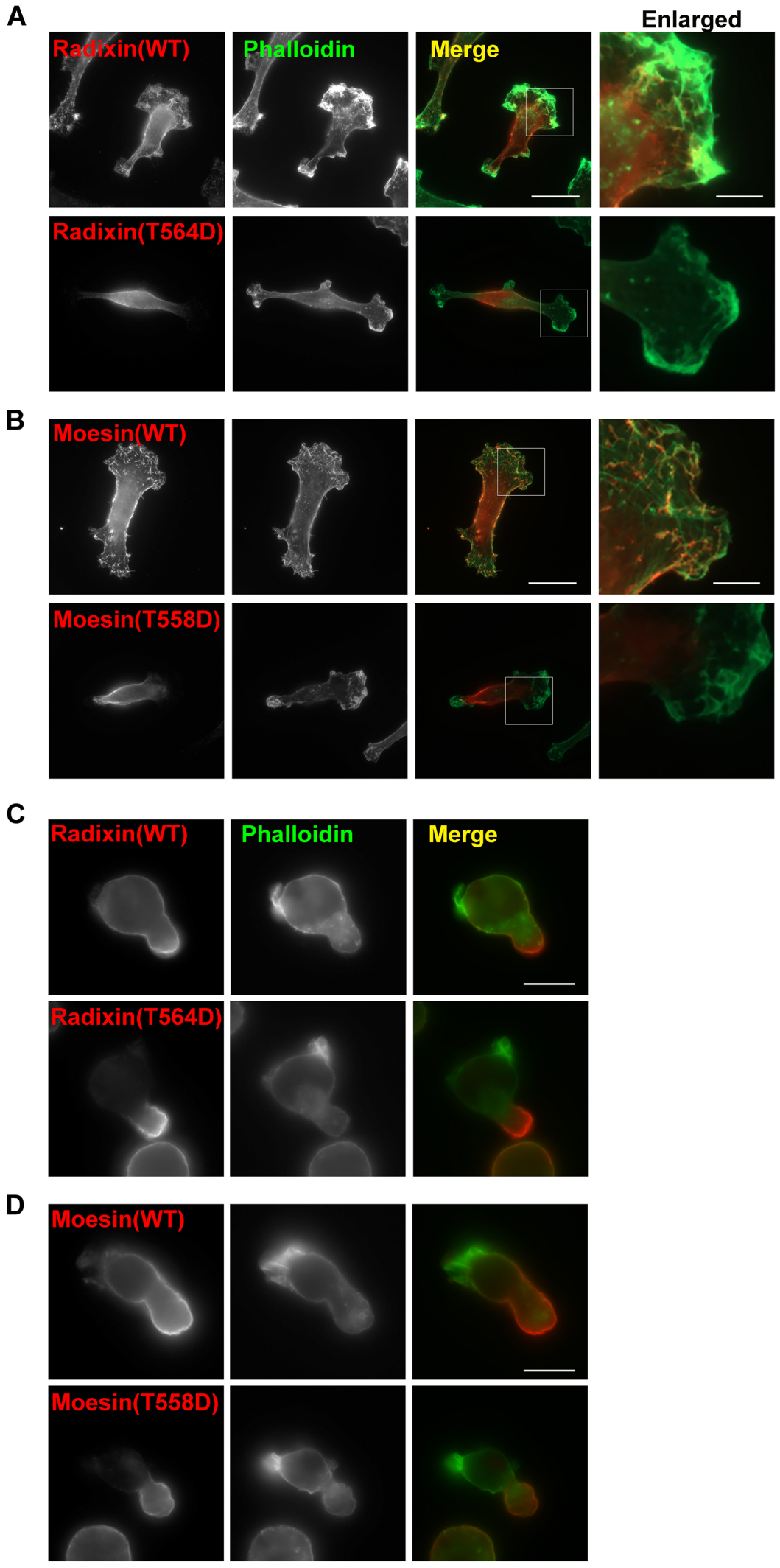

Supplementary Figure S4 Inoue & Takatsu

Fig. S4. Polarized localization of the phosphomimetic radixin and moesin mutants. (A, B) MDA-MB-231 cells and **(C, D)** BaF3 cells stably expressing C-terminally FLAG-tagged radixin(WT), radixin(T564D), moesin(WT), or moesin(T558D) were fixed and stained for FLAG followed by incubation with Alexa555-conjugated anti-mouse secondary antibody and Alexa488-conjugated phalloidin. Scale bars, 20 μm, 5 μm in enlarged images **(A, B)**, and 10 μm **(C, D)**.

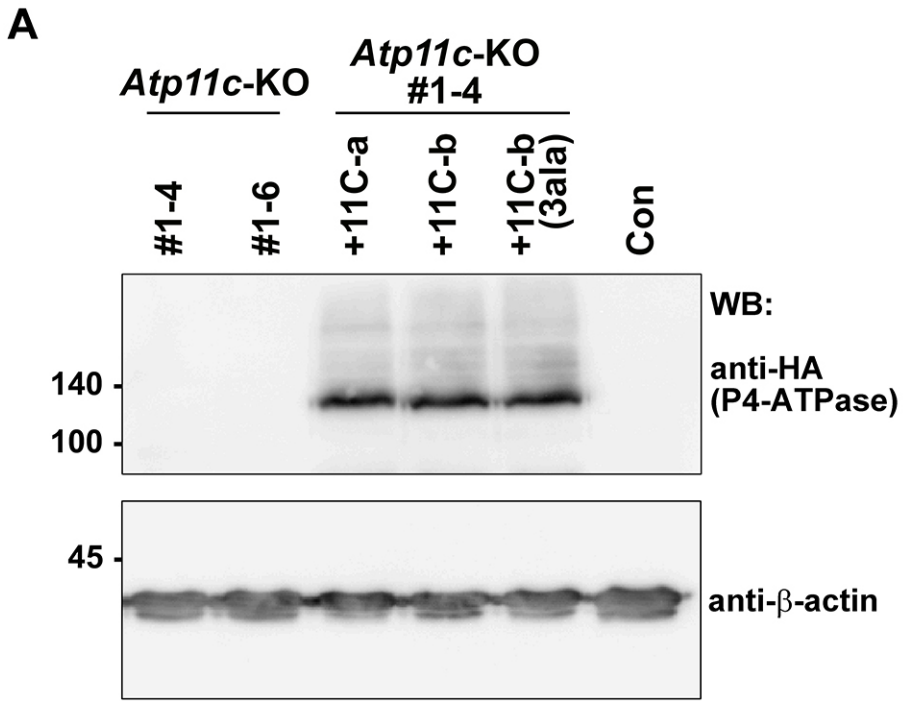

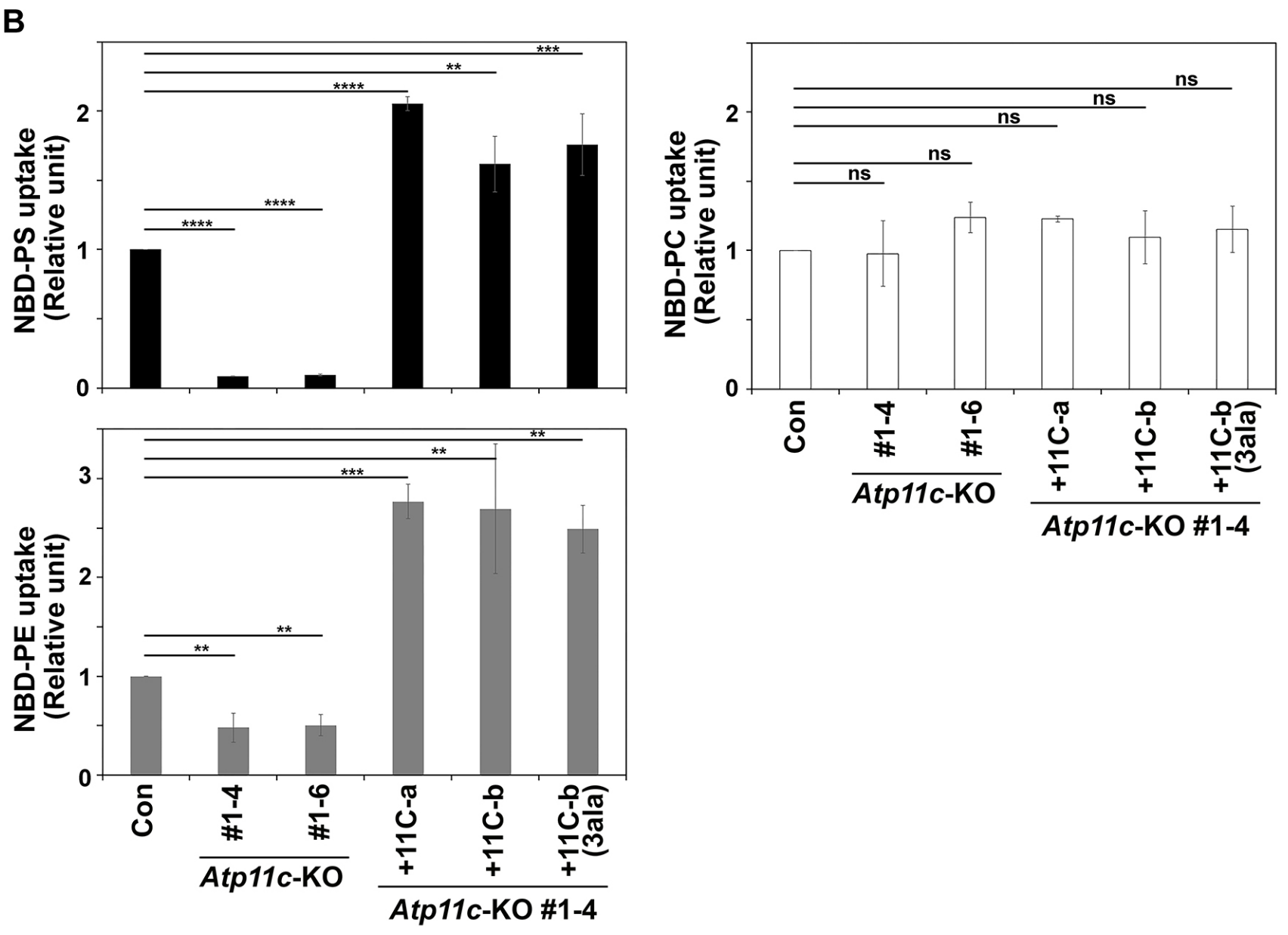

Supplementary Figure S5 Inoue & Takatsu

Fig. S5. Expression of exogenous ATP11C-a, ATP11C-b, and ATP11C-b(3ala) in *Atp11c*-knockout cells. (A) Parental BaF3 cells (Con), *Atp11c*-knockout cells, and cells stably expressing CRISPR-resistant HA-tagged ATP11C-a, ATP11C-b, or ATP11C-b(3ala) in the indicated *Atp11c*-knockout cell clone were lysed, and lysates were subjected to SDS-PAGE and immunoblotting using anti-HA or anti-β-actin (as an internal control) antibodies. **(B)** Cells in **(A)** were washed with flippase assay buffer and incubated with NBD-PS for 5 min, NBD-PE for 15 min, or NBD-PC for 15 min at 15°C. After extraction with fatty acid-free BSA, cellular fluorescence intensity was measured by flow cytometry. Uptake of NBD-conjugated lipids is shown relative to parental cells (Con). Graphs ± SD display the average of three independent experiments. A one-way ANOVA was performed to assess variance, and comparisons to parental cells (Con) were made with Dunnett's analysis. ** $p < 0.01$, *** $p < 0.001$, **** $p < 0.0001$.

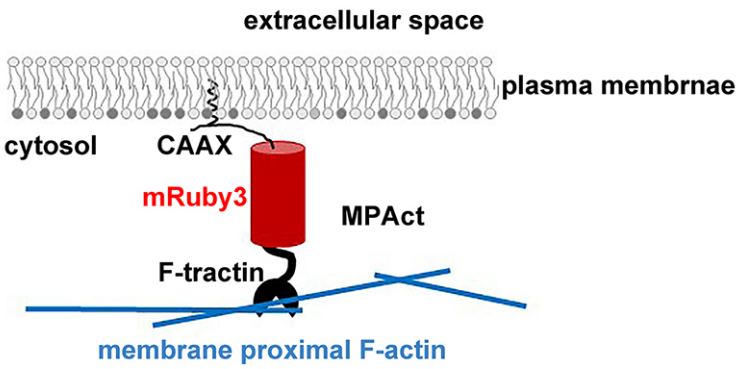

Fig. S6. MPAct probe recognizes membrane proximal F-actin (Bisaria et al., 2020)

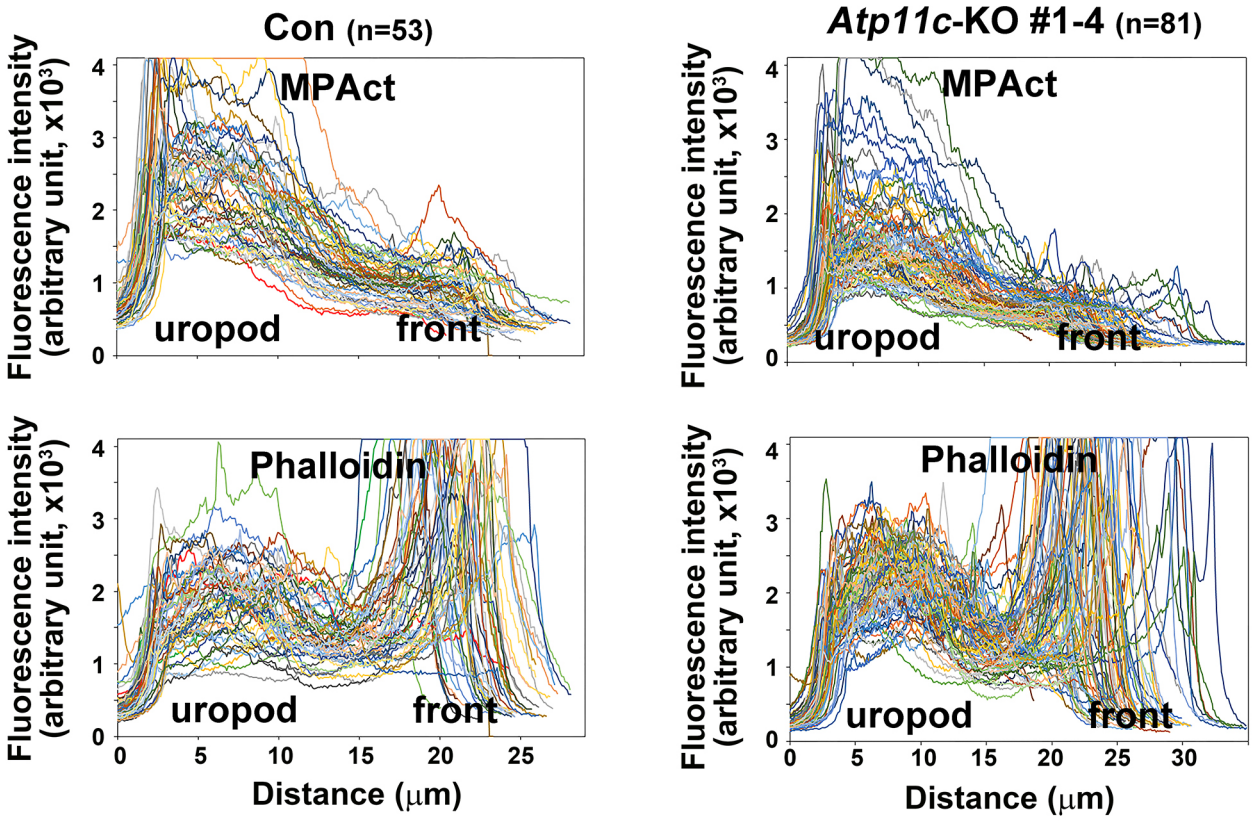

Supplementary Figure S7 Inoue & Takatsu

Fig. S7. Enrichment of MPAct at the uropod in BaF3 cells

Parental BaF3 cells (Con) and *Atp11c*-knockout cells stably expressing MPAct-mRuby3 were fixed and incubated with Alexa488-conjugated phalloidin. Line-scan profiles of MPAct and phalloidin fluorescence from the uropod to the front of these cells are shown. Different colors of lines represent different cells and 'n' is the total number of analyzed cells.